

Dynamic properties of rumor propagation model induced by Lévy noise on social networks

Ying Jing(景颖), Youguo Wang(王友国), Qiqing Zhai(翟其清), and Xianli Sun(孙先莉)

Citation: Chin. Phys. B, 2024, 33 (**9**): 090203. DOI: 10.1088/1674-1056/ad58c5
Journal homepage: http://cpb.iphy.ac.cn; http://iopscience.iop.org/cpb

What follows is a list of articles you may be interested in

An improved ISR-WV rumor propagation model based on multichannels with time delay and pulse vaccination

Yafang Dong(董雅芳), Liangán Huo(霍良安), Xiaoxiao Xie(谢笑笑), and Ming Li(李明)
Chin. Phys. B, 2023, 32 (**7**): 070205. DOI: 10.1088/1674-1056/acd2be

Ergodic stationary distribution of a stochastic rumor propagation model with general incidence function

Yuhuai Zhang(张宇槐) and Jianjun Zhu(朱建军)
Chin. Phys. B, 2022, 31 (**6**): 060202. DOI: 10.1088/1674-1056/ac48fa

Correlation and trust mechanism-based rumor propagation model in complex social networks

Xian-Li Sun(孙先莉), You-Guo Wang(王友国), and Lin-Qing Cang(仓林青)
Chin. Phys. B, 2022, 31 (**5**): 050202. DOI: 10.1088/1674-1056/ac3d82

Dynamics and intermittent stochastic stabilization of a rumor spreading model with guidance mechanism in heterogeneous network

Xiaojing Zhong(钟晓静), Yukun Yang(杨宇琨), Runqing Miao(苗润青), Yuqing Peng(彭雨晴), and Guiyun Liu(刘贵云)
Chin. Phys. B, 2022, 31 (**4**): 040205. DOI: 10.1088/1674-1056/ac587d

Dynamics and near-optimal control in a stochastic rumor propagation model incorporating media coverage and Lévy noise

Liang'an Huo(霍良安) and Yafang Dong(董雅芳)
Chin. Phys. B, 2022, 31 (**3**): 030202. DOI: 10.1088/1674-1056/ac2f35

Dynamic properties of rumor propagation model induced by Lévy noise on social networks

Ying Jing(景颖)[1], Youguo Wang(王友国)[1,†], Qiqing Zhai(翟其清)[1], and Xianli Sun(孙先莉)[2]

[1] *School of Science, Nanjing University of Posts and Telecommunications, Nanjing* 210023, *China*
[2] *School of Telecommunication and Information Engineering, Nanjing University of Posts and Telecommunications, Nanjing* 210023, *China*

(Received 25 March 2024; revised manuscript received 2 June 2024; accepted manuscript online 17 June 2024)

Social networks are inevitably subject to disruptions from the physical world, such as sudden internet outages that sever local connections and impede information flow. While Gaussian white noise, commonly used to simulate stochastic disruptions, only fluctuates within a narrow range around its mean and fails to capture large-scale variations, Lévy noise can effectively compensate for this limitation. Therefore, a susceptible–infected–removed rumor propagation model with Lévy noise is constructed on homogeneous and heterogeneous networks, respectively. Then, the existence of a global positive solution and the asymptotic path-wise of the solution are derived on heterogeneous networks, and the sufficient conditions of rumor extinction and persistence are investigated. Subsequently, theoretical results are verified through numerical calculations and the sensitivity analysis related to the threshold is conducted on the model parameters. Through simulation experiments on Watts–Strogatz (WS) and Barabási–Albert networks, it is found that the addition of noise can inhibit the spread of rumors, resulting in a stochastic resonance phenomenon, and the optimal noise intensity is obtained on the WS network. The validity of the model is verified on three real datasets by particle swarm optimization algorithm.

Keywords: rumor propagation model, Lévy noise, extinction and persistence, stochastic resonance

PACS: 02.50.Ey, 02.50.Fz, 64.60.aq, 87.23.Kg **DOI:** 10.1088/1674-1056/ad58c5

1. Introduction

Stochastic disturbances (e.g., uncertain factors including time, climate, or environment during disease diffusion) can lead to the destabilization of systems. Accordingly, it is necessary to consider the impact of random interference on the entire system.[1–3] Many experts and scholars have already taken environmental disturbance into account in nonlinear systems.[4–7] Mao and Marion added environmental noise to deterministic systems and found that even tiny amounts of Gaussian white noise can suppress potential population explosions.[8] Jiang *et al*. investigated a unique global positive solution and its asymptotic behavior on a stochastic model.[9] Zhu and Wang introduced the stochastic disturbances into the connected degree of a fixed-scale network. They found that adding interval Gaussian white noise facilitates the spread of rumors, namely, stochastic resonance occurs.[10] Based on this, Chai and Wang presented the variation of network scale, effected by stochastic perturbations represented by Gaussian white noise, then proposed a stochastic information diffusion model considering both connectivity interference and population perturbations.[11] Tong *et al*. researched the dynamic properties of a rumor propagation model driven by Gaussian white noise on heterogeneous networks under the background of MicroBlog.[12]

Unfortunately, representing population disturbances with Gaussian white noise is sometimes not applicable when populations are affected by emergencies.[13] Gaussian white noise only idealizes the actual random noise and can only fluctuate around a small range near the mean, unable to simulate large-scale fluctuations. However, Lévy noise exhibits long-tailed characteristics and can effectively simulate wide-ranging fluctuations, which is more conducive to reflecting the random perturbation in the objective reality.[14] Bao and Yuan introduced Lévy process to capture the potential population dynamics. They found that Lévy noise can also suppress population explosion.[15] Zhou *et al.* discussed the threshold of a stochastic epidemic model with Lévy noise to judge when the rumor vanishes or prevails.[16] Privault and Wang replaced Burkholder–Davis–Gundy inequality with Kunita's inequality and obtained the threshold of susceptible–infected–removed (SIR) model with infinite Lévy measure.[17] Huo *et al*. obtained the dynamic properties around the rumor-free equilibrium and the rumor endemic equilibrium,[18] and investigated the control strategy of a stochastic rumor diffusion model with media coverage and Lévy noise.[19]

Furthermore, stochastic resonance, which appeared in a rumor propagation stochastic model as mentioned in Ref. [10], refers to a counterintuitive phenomenon observed in certain nonlinear systems, where noise actually enhances the response of systems and plays a critical role in optimizing performance.[20] Liu *et al*. researched the stochastic resonance of a mono-threshold system with additive noise and multiplicative noise, exploring the effect of system threshold and noise intensity on the detection.[21] Guo *et al*. investigated the

†Corresponding author. E-mail: wangyg@njupt.edu.cn

© 2024 Chinese Physical Society and IOP Publishing Ltd

stochastic resonance driven by multiplicative Gaussian white noise and additive Lévy noise in FitzHugh–Nagumo neural system. They discussed the effect of signal-noise-ratio on different system parameters.[22]

Considering that unexpected events such as regional network outages or the sudden rise of a topic can lead to a sudden decrease or increase in the number of nodes accessing the network, which is more in line with the characteristics of the Lévy distribution, we establish a rumor propagation model driven by Lévy noise. Currently, stochastic resonance has been observed in many nonlinear systems.[23,24] However, there is limited research on the occurrence of stochastic resonance in a rumor propagation stochastic model. This article will explore whether the stochastic resonance phenomenon occurs in the proposed stochastic model. The main achievements of this paper are as follows.

(1) Considering the environmental disturbance of the inflow rate on the scale of network, we use Lévy noise to describe this distribution of nodes inflow rate, a stochastic model driven by Lévy noise is proposed on homogeneous and heterogeneous networks.

(2) In the context of heterogeneous networks, the threshold $\tilde{R}_0$ of rumor extinction and the threshold $\tilde{R}_0$ of persistence are deduced. $\tilde{R}_0 < 1$ inflects the rumor will tend to vanish, whereas $\tilde{R}_0 > 1$ means the rumor will continue prevailing.

(3) Considering that the degree of network nodes follows a power-law distribution, the numerical scheme of the SIR model induced by Lévy noise on heterogeneous networks is given by Milstein method. Meanwhile, sensitivity analysis is conducted and the results are presented in graphical form.

(4) We select two indexes, i.e., peak density of infected nodes and life cycle of rumor, to describe the characteristics of this propagation model. The effects of different noise intensities on them are illustrated by simulation. Subsequently, the optimal noise is searched on homogeneous networks to determine the minimum of both peak density of infected nodes and life cycle of rumor.

The structure of this paper is organized as follows. In Section 2, an improved SIR rumor propagation model with Lévy noise is established on homogeneous and heterogeneous networks. In Section 3, the globally unique solution of this stochastic model is proved on heterogeneous networks. The calculation of the asymptotic path-wise for the solution is discussed and the sufficient conditions of the rumor extinction and persistence are derived on heterogeneous networks. In Section 4, the numerical simulations on artificial networks and sensitivity analysis are conducted. In addition, the influences of different noise intensities on rumor diffusion and the optimal noise intensities are discussed. The effectiveness of the proposed model is validated through real datasets.

2. Theoretical model

In this section, we construct a rumor diffusion model on homogeneous and heterogeneous networks, respectively. The description of homogeneous and heterogeneous networks needs to be briefly introduced in advance.

In homogeneous networks, the distribution of node degrees is relatively uniform, which means that most nodes have a similar number of connections. In heterogeneous networks, the distribution of node degrees is very uneven and usually follows a power-law distribution; namely, a few nodes (referred to as hub nodes or important nodes) have many connections, while the majority of nodes have only a few connections. More graphically, two typical examples of homogeneous and heterogeneous networks, as Watts–Strogatz (WS) and Barabási–Albert (BA) networks, are displayed in Fig. 1. By comparison, the BA network fully reflects the existence of hub nodes.

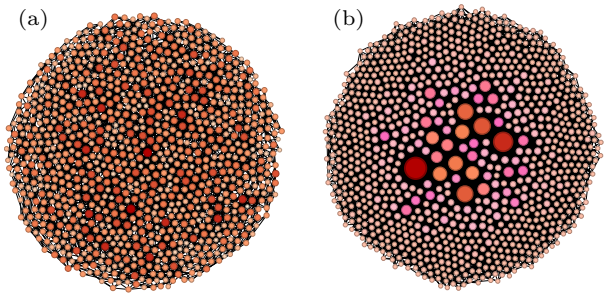


Fig. 1. Topology diagrams of (a) WS networks and (b) BA networks.

The outflow rate of nodes increases slowly compared to the life cycle of rumors. Considering the variation of outflow rate affected by emergencies, the network scale $N(t)$ is subjected to time-dependent changes.[11] At each time step, nodes are categorized into three types: susceptible nodes (S), infected nodes (I), and removed nodes (R). In particular, susceptible nodes refer to nodes that have never been exposed to the rumor. Infected nodes refer to nodes that, after being exposed to the rumor, choose to believe and propagate it. Removed nodes are nodes that know rumors but stop spreading them.

Since most nodes have a similar number of degrees in homogeneous networks, we assume that each node has an average of neighboring nodes $\langle k \rangle$. However, in heterogeneous networks, due to the power-law distribution of node degrees and the significant impact of hub nodes on information propagation, we assume that nodes in the network have various degrees $k = 1, 2, \ldots, n$. Thus, nodes with the same degree are grouped according to their different states, regarding as S_k, I_k, and R_k $(k = 1, 2, \ldots, n)$. For instance, the density of I-state nodes with the same degree 1 are grouped as I_1. Thereby, the nodes of three states are divided as n groups in heterogeneous networks.

2.1. Deterministic model

The S_k, I_k, and R_k $(k = 1,2,\ldots,n)$ adhere to the rules as below, and the corresponding notations are described in Table 1. At every time step, there is a natural inflow volume A nodes join to the S_k-state, while the nodes of S_k-state will leave the network by a probability η. S_k turns to I_k when the S_k node believes and spreads the rumor with probability β. I_k turns to R_k when the I_k node does not spread the rumor with probability μ.

Table 1. The interpretation of notations.

Variable	Notations description
A	the inflow volume
η	the outflow rate
β	the infected rate
μ	the removed rate

In view of the homogenous mixing hypothesis[10] and Fig. 2, the mean-field equation of the deterministic SIR rumor propagation model on heterogeneous networks is given by

$$\begin{cases} \dfrac{\mathrm{d}S_k(t)}{\mathrm{d}t} = A - \beta k S_k(t)\Theta(t) - \eta S_k(t), \\ \dfrac{\mathrm{d}I_k(t)}{\mathrm{d}t} = \beta k S_k(t)\Theta(t) - (\mu+\eta) I_k(t), \\ \dfrac{\mathrm{d}R_k(t)}{\mathrm{d}t} = \mu I_k(t) - \eta R_k(t), \end{cases} \tag{1}$$

where

$$\Theta(t) = \sum_{k'} I_{k'}(t) P(k'|k) = \frac{1}{\langle k\rangle}\left(\sum_{k'} k' I_{k'}(t) P(k')\right)$$

represents the probability of a given node with degree k having an infected node k' with degree among its neighbors at time t.[10,25]

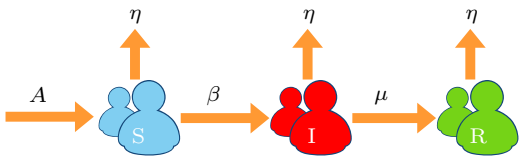


Fig. 2. Structure of the deterministic SIR rumor propagation model.

The rumor-free equilibrium point of model (1) can easily be obtained as $E_0 = (A/\eta, 0, 0, \ldots, A/\eta, 0, 0)$. Let $E^* = (S_k^*, I_k^*, R_k^*)$ $(k = 1,2,\ldots,n)$ be the rumor endemic equilibrium point. Then, $S_k^* = \frac{A}{\eta+\beta k\Theta^*}$, $I_k^* = \frac{\beta k A\Theta^*}{(\mu+\eta)(\eta+\beta k\Theta^*)}$, $R_k^* = \frac{\mu\beta k A\Theta^*}{\eta(\mu+\eta)(\eta+\beta k\Theta^*)}$. Substitute I_k^* into $\Theta^*(t)$, then

$$\Theta^* = \frac{1}{\langle k\rangle}\sum_{i=1}^{n} iP(i)\frac{\beta i A\Theta^*}{(\mu+\eta)(\eta+\beta i\Theta^*)}.$$

Subsequently, the root located theorem will be utilized to prove the existence and uniqueness of endemic equilibrium points. Define a function as

$$f(\Theta^*) = \frac{1}{\langle k\rangle}\sum_{i=1}^{n} iP(i)\frac{\beta i A\Theta^*}{(\mu+\eta)(\eta+\beta i\Theta^*)} - \Theta^*. \tag{2}$$

Obviously, $\Theta^* = 0$ is a solution of Eq. (2) and

$$f(1) = \frac{1}{\langle k\rangle}\sum_{i=1}^{n} iP(i)\frac{\beta i A}{(\mu+\eta)(\eta+\beta i)} - 1 > 0.$$

To sure $\Theta^* \in (0,1)$, the following inequality must be satisfied:

$$\begin{aligned} \frac{\mathrm{d}f(\Theta^*)}{\mathrm{d}\Theta^*}|_{\Theta^*=0} &= \frac{1}{\langle k\rangle}\frac{\beta A}{\mu+\eta}\sum_{i=1}^{n} i^2 P(i)\frac{\eta}{(\eta+\beta i\Theta^*)^2} - 1\,|_{\Theta^*=0} \\ &= \frac{1}{\langle k\rangle}\frac{\beta A}{\mu+\eta}\sum_{i=1}^{n} i^2 P(i)\frac{1}{\eta} - 1 \\ &= \frac{\langle k^2\rangle}{\langle k\rangle}\frac{\beta A}{\eta(\mu+\eta)} - 1 > 0. \end{aligned}$$

Thus, $R_0 = \frac{\langle k^2\rangle}{\langle k\rangle}\frac{\beta A}{\eta(\mu+\eta)}$ is the threshold (basic reproductive number), which implies that model (1) has a unique rumor endemic equilibrium point E^* while $R_0 > 1$.

Remark 1 It is easy to discover that R_0, related to $\langle k^2\rangle/\langle k\rangle$, describes the heterogeneity of the network.

2.2. Stochastic model

The scale of a network is easily influenced by emergencies, such as regional internet outages or the sudden popularity of a particular topic, which lead to a sudden decrease or increase in the number of network nodes. Notice that these emergencies occur rapidly and have a wide-ranging impact, which aligns with the characteristics of the Lévy distribution.[15] On the other hand, Lévy noise combines Brown motion with jump processes, providing a model to describe both continuous and discontinuous random fluctuations. Compared with Ref. [11], Gaussian white noise is suitable for normal interference, and Lévy noise is suitable for sudden interference. Since the impact of random interference on each node is different, we will denote $L_i(t) = \sigma_i B_i(t) + \int_0^t\int_Z \gamma_i(u)\tilde{N}(\mathrm{d}s,\mathrm{d}u)$, $i = 1,2,3$ on a measurable subset Z of $[0,\infty)$ to represent the Lévy noise, where B_i $(i = 1,2,3)$ is the standard Brownian motion with independent stationary increments and noise intensity σ_i $(i = 1,2,3)$. $\gamma_i(u) > -1, u \in Z$, $i = 1,2,3$ represents the intensity of jump which is bounded and continuous. $\tilde{N}(\mathrm{d}t,\mathrm{d}u) = N(\mathrm{d}t,\mathrm{d}u) - \nu(\mathrm{d}u)\mathrm{d}t$ represents the compensated Poisson random measure with the Poisson counting measure $N(\mathrm{d}t,\mathrm{d}u)$ and the characteristic measure $\nu(Z) < \infty$. Note that all the stochastic processes involved in this paper are defined on a complete filtered probability space $(\Omega,\Im,(\Im_t)_{t\geq 0},P)$, where $\{\Im_t\}_{t\geq 0}$ is right continuous and $\Im_0$ contains all $\mathbb{P}$-null sets. Thus, the variation of outflow rate can be described as $\eta \to \eta - \dot{L}_i(t)$. $\eta - \dot{L}_i(t)$ can be understood as the reduction rate of nodes affected by noise interference while $\eta - \dot{L}_i(t) > 0$, while it can be understood as the additional inflow rate of nodes if $\eta - \dot{L}_i(t) < 0$. The propagation process diagram of the stochastic SIR model is displayed in Fig. 3.

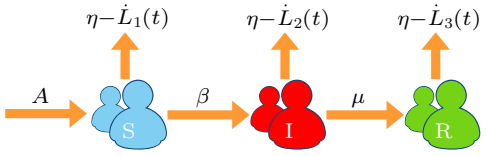


Fig. 3. Structure of the stochastic SIR rumor propagation model.

2.2.1. Homogeneous network

Based on Fig. 3, the mean-field equation of rumor spreading model driven by Lévy noise on homogeneous networks can be established as below:

$$\begin{cases} \mathrm{d}S(t) = (A-\beta\langle k\rangle S(t)I(t)-\eta S(t))\,\mathrm{d}t + S(t)\,\mathrm{d}L_1(t), \\ \mathrm{d}I(t) = (\beta\langle k\rangle S(t)I(t)-(\mu+\eta)I(t))\,\mathrm{d}t + I(t)\,\mathrm{d}L_2(t), \\ \mathrm{d}R(t) = (\mu I(t)-\eta R(t))\,\mathrm{d}t + R(t)\,\mathrm{d}L_3(t), \end{cases} \tag{3}$$

where, $S(t)$, $I(t)$, $R(t)$ represent the number of nodes in each state at time t, respectively. Meanwhile, $S(t)+I(t)+R(t)=N(t)$. $S(0)$, $I(0)$ and $R(0)$ are the initial condition of $S(t)$, $I(t)$ and $R(t)$ when $t=0$.

2.2.2. Heterogeneous network

Considering the heterogeneity of social networks, the mean-field equation of the SIR rumor diffusion model induced by Lévy noise is established as below:

$$\begin{cases} \mathrm{d}S_k(t) = [A-\beta kS_k(t)\Theta(t)-\eta S_k(t)]\,\mathrm{d}t + S_k(t)\,\mathrm{d}L_1(t), \\ \mathrm{d}I_k(t) = [\beta kS_k(t)\Theta(t)-(\mu+\eta)I_k(t)]\,\mathrm{d}t + I_k(t)\,\mathrm{d}L_2(t), \\ \mathrm{d}R_k(t) = [\mu I_k(t)-\eta R_k(t)]\,\mathrm{d}t + R_k(t)\,\mathrm{d}L_3(t). \end{cases} \tag{4}$$

3. Theoretical analysis

Most researches on the dynamics of stochastic information propagation models have been conducted on homogeneous networks. The focus will now shift to exploring the dynamic properties of the proposed SIR model induced by Lévy noise on heterogeneous networks. Due to the reliance on known information for rumor dissemination, there is no aftereffect. Mathematically, there exists $D_m>0$ $(m>0)$ such that

(H1) $\int_Z |H(x,u)-H(x,u)|^2 v(\mathrm{d}u) \le D_m|x-y|^2$ $(u\in Z)$, where $H(x,u)=\gamma(u)x(t)$ with $|x|\vee|y|\le m$.

(H2) $|\ln(1+\gamma(u))|\le C$, for $\gamma(u)>-1$, where C is a positive constant, $u\in Z$.

3.1. Existence and uniqueness of global solution

Lemma 1[18] **(Lévy–Itô formula)** A given stochastic differential equation is as follows:

$$\mathrm{d}X = F(t,X(t))\,\mathrm{d}t + G(t,X(t))\,\mathrm{d}B(t) + \int_Z H(t,X(t))\tilde{N}(\mathrm{d}t,\mathrm{d}u).$$

If L is an operator of $\Phi\in C^{1,2}(\mathbb{R}_+\times\mathbb{R}_+^3)$, then

$$\begin{aligned}\mathrm{d}\Phi(X(t)) &= L\Phi(X(t))\,\mathrm{d}t + \Phi_x(X(t))G(t,x)\,\mathrm{d}B(t) \\ &\quad + \int_Z [\Phi(X(t)+H(t,u))-\Phi(X(t))]\tilde{N}(\mathrm{d}t,\mathrm{d}u),\end{aligned}$$

which is called the Lévy–Itô formula, and

$$\begin{aligned}L\Phi(X(t)) &= \Phi_x(X(t))F(t,x) \\ &\quad + \frac{1}{2}\mathrm{trace}\left[G^{\mathrm{T}}(t,X(t))\Phi_{xx}G(t,X(t))\right] \\ &\quad + \int_Z [\Phi(X(t)+H(t,u))-\Phi(X(t)) \\ &\quad - \Phi_x(X(t))H(t,u)]v(\mathrm{d}u).\end{aligned}$$

Here $\Phi_x=\left(\frac{\partial\Phi}{\partial x_1},\frac{\partial\Phi}{\partial x_2},\frac{\partial\Phi}{\partial x_3}\right)$, $\Phi_{xx}=\left(\frac{\partial^2\Phi}{\partial x_i\partial x_j}\right)_{3\times3}$.

Theorem 1 Under the assumptions (H1) and (H2), if model (4) has the initial value $(S_1(0), I_1(0), R_1(0),\ldots, S_n(0), I_n(0), R_n(0))\in\mathbb{R}_+^{3n}$, then for any $t\ge0$, there exists a unique solution within $\mathbb{R}_+^{3n}$.

Proof Define the moment of explosion as τ_e. The coefficients of model (4) satisfy the locally Lipschitz and linear growth condition, leading to the existence of a locally unique solution $(S_1(t),I_1(t),R_1(t),\ldots,S_n(t),I_n(t),R_n(t))\in\mathbb{R}_+^{3n}$ under $[0,\tau_\mathrm{e})$. To make sure the globality of $(S_1(t), I_1(t), R_1(t),\ldots, S_n(t), I_n(t), R_n(t))$, $\tau_\mathrm{e}=\infty a.e.$ must be demonstrated. Assuming the existence of a sufficiently large constant $m_0>0$, so that $S_k(t),I_k(t),R_k(t)\in[1/m_0,m_0]$ for any $k=1,2,\ldots,n$ and $m\ge m_0$. Define the stopping time τ_m as

$$\begin{aligned}\tau_m &= \inf\{t\in[0,\tau_\mathrm{e}) : \min\{S_k(t),I_k(t),R_k(t)\}\le 1/m \text{ or} \\ &\quad \max\{S_k(t),I_k(t),R_k(t)\}\ge m\}.\end{aligned}$$

It is evident that $\{\tau_m\}$ is a monotonically increasing sequence. Let $\tau_\infty=\lim\limits_{m\to\infty}\tau_m$, then $\tau_\infty\le\tau_\mathrm{e}\,a.e.$ Suppose that $\tau_\infty=\infty a.e.$, then the presence of $T>0$ and $\varepsilon\in(0,1)$ results in $P\{\tau_\infty\le T\}\ge\varepsilon$. Therefore, $P\{\tau_m\le T\}\ge\varepsilon$ exists for any integer $m\ge m_0$.

Define a function $V(x):\mathbb{R}_+^{3n}\to\mathbb{R}_+$ as

$$\begin{aligned}&V(S_1(t),I_1(t),R_1(t),\ldots,S_n(t),I_n(t),R_n(t)) \\ &= \sum_{k=1}^{n}\left[\begin{matrix}S_k(t)-a-a\ln\frac{S_k(t)}{a}+I_k(t)-1 \\ -\ln I_k(t)+R_k(t)-1-\ln R_k(t)\end{matrix}\right],\end{aligned}$$

here $a=2\langle k\rangle\eta/[\beta n^2(n+1)\max\limits_{1\le k\le n}P(k)]$. Utilizing Lemma 1,

$$\begin{aligned}\mathrm{d}V &= LV\,\mathrm{d}t + \sum_{k=1}^{n}\Big\{(S_k(t)-a)\sigma_1\,\mathrm{d}B_1(t)+(I_k(t)-1)\sigma_2\,\mathrm{d}B_2(t)+(R_k(t)-1)\sigma_3\,\mathrm{d}B_3(t) \\ &\quad + \int_Z[\gamma_1(u)S_k(t)+\gamma_2(u)I_k(t)+\gamma_3(u)R_k(t)-a\ln(1+\gamma_1(u))-\ln(1+\gamma_2(u))(1+\gamma_3(u))]\tilde{N}(\mathrm{d}t,\mathrm{d}u)\Big\},\end{aligned}$$

herein,

$$\begin{aligned} LV \leq & \sum_{k=1}^{n}\Bigg\{A+\mu+(a+2)\eta+a\beta k\Theta(t)-\eta I_k(t)+\frac{a\sigma_1^2+\sigma_2^2+\sigma_3^2}{2} \\ & +\int_Z\left[a\left(\gamma_1(u)-\ln(1+\gamma_1(u))\right)+\gamma_2(u)+\gamma_3(u)-\ln(1+\gamma_2(u))(1+\gamma_3(u))\right]v(\mathrm{d}u)\Bigg\} \\ \leq & \sum_{k=1}^{n}\Bigg\{A+\mu+(a+2)\eta+\left(\frac{a\beta kn^2(n+1)\underset{1\leq k\leq n}{\max}P(k)}{2\langle k\rangle}-\eta\right)I_k(t)+\frac{a\sigma_1^2+\sigma_2^2+\sigma_3^2}{2} \\ & +\int_Z\left[a\left(\gamma_1(u)-\ln(1+\gamma_1(u))\right)+\gamma_2(u)+\gamma_3(u)-\ln(1+\gamma_2(u))(1+\gamma_3(u))\right]v(\mathrm{d}u)\Bigg\} \\ = & \sum_{k=1}^{n}\Bigg\{A+\mu+(a+2)\eta+\frac{a\sigma_1^2+\sigma_2^2+\sigma_3^2}{2} \\ & +\int_Z\left[a\left(\gamma_1(u)-\ln(1+\gamma_1(u))\right)+\gamma_2(u)+\gamma_3(u)-\ln(1+\gamma_2(u))(1+\gamma_3(u))\right]v(\mathrm{d}u)\Bigg\} \\ := & M_1 \end{aligned}$$

yields

$$\begin{aligned} \mathrm{d}V \leq & M_1\,\mathrm{d}t+\sum_{k=1}^{n}\Bigg\{(S_k(t)-a)\,\sigma_1\,\mathrm{d}B_1(t)+(I_k(t)-1)\,\sigma_2\,\mathrm{d}B_2(t)+(R_k(t)-1)\,\sigma_3\,\mathrm{d}B_3(t) \\ & +\int_Z\left[\gamma_1(u)S_k(t)+\gamma_2(u)I_k(t)+\gamma_3(u)R_k(t)-a\ln(1+\gamma_1(u))-\ln(1+\gamma_2(u))(1+\gamma_3(u))\right]\tilde{N}(\mathrm{d}t,\mathrm{d}u)\Bigg\}. \end{aligned} \tag{5}$$

Integrating Eq. (5) from 0 to $\tau_m\wedge T$ results in

$$\begin{aligned} \int_0^{\tau_m\wedge T}\mathrm{d}V \leq & \int_0^{\tau_m\wedge T}M_1\,\mathrm{d}t+\int_0^{\tau_m\wedge T}\sum_{k=1}^{n}\Bigg\{(S_k(t)-a)\,\sigma_1\,\mathrm{d}B_1(t)+(I_k(t)-1)\,\sigma_2\,\mathrm{d}B_2(t)+(R_k(t)-1)\,\sigma_3\,\mathrm{d}B_3(t) \\ & +\int_Z\left[\gamma_1(u)S_k(t)+\gamma_2(u)I_k(t)+\gamma_3(u)R_k(t)-a\ln(1+\gamma_1(u))-\ln(1+\gamma_2(u))(1+\gamma_3(u))\right]\tilde{N}(\mathrm{d}t,\mathrm{d}u)\Bigg\}. \end{aligned}$$

Then, take the expectation on both sides,

$$\begin{aligned} 0 \leq & E\left[V\left(S_1(\tau_m\wedge T),I_1(\tau_m\wedge T),R_1(\tau_m\wedge T),\ldots,S_n(\tau_m\wedge T),I_n(\tau_m\wedge T),R_n(\tau_m\wedge T)\right)\right] \\ \leq & E\left[V\left(S_1(0),I_1(0),R_1(0),\ldots,S_n(0),I_n(0),R_n(0)\right)\right]+M_1T. \end{aligned}$$

Given a function $D(h)$ and $\lim\limits_{h\to\infty}D(h)=\infty$, for any $h>0$,

$$D(h)=\inf\left\{\begin{array}{l}V\left(S_1(t),I_1(t),R_1(t),\ldots,S_n(t),I_n(t),R_n(t)\right):\min\{S_k(t),I_k(t),R_k(t)\}\leq 1/m\\ \text{or}\ \ \max\{S_k(t),I_k(t),R_k(t)\}\geq m,\ \ k=1,2,\ldots,n\end{array}\right\}.$$

Then, a contradiction

$$\begin{aligned} \infty > & E[V(S_1(0),I_1(0),R_1(0),\ldots,S_n(0),I_n(0),R_n(0))] \\ & +M_1T=\infty \end{aligned}$$

arises, as $k\to\infty$. Thus, the appearance of $\tau_e=\infty a.e.$ causes the existence and uniqueness of global solution.

3.2. Asymptotic path-wise estimation

Lemma 2[26] **(strong law of large numbers)** Let $M=\{M(t)\}_{t\geq 0}$ be a real-values continuous local martingale vanishing at $t=0$. Then

$$\lim_{t\to\infty}\langle M,M\rangle(t)=\infty\ \ a.s.\ \ \Rightarrow$$

$$\lim_{t\to\infty}\frac{M(t)}{\langle M,M\rangle(t)}=0\ \ a.s.,$$

and also

$$\limsup_{t\to\infty}\frac{\langle M,M\rangle(t)}{t}<\infty\ \ a.s.\ \ \Rightarrow$$

$$\lim_{t\to\infty}\frac{M(t)}{t}=0\ \ a.s.$$

Theorem 2 For any $k=1,2,\ldots n$, if $(S_k(t),I_k(t),R_k(t))\in\mathbb{R}_+^{3n}$ is the solution of model (4) with initial value $(S_k(0),I_k(0),R_k(0))\in\mathbb{R}_+^{3n}$. Denote $X_k(t)=S_k(t)+I_k(t)+R_k(t)$, then

$$\lim_{t\to\infty}\frac{X_k(t)}{t}=0\quad P-a.s.$$

Proof Constructing a function as $V(X_k(t)) = X_k^p(t)$ $(p > 2,\ k = 1,2,\ldots,n)$, by means of Lemma 1, there is

$$\begin{aligned} \mathrm{d}V(X_k(t)) \;=\; & LV\,\mathrm{d}t + pX_k^{p-1}(t)\big(\sigma_1 S_k\,\mathrm{d}B_1(t) \\ & + \sigma_2 I_k\,\mathrm{d}B_2(t) + \sigma_3 R_k\,\mathrm{d}B_3(t)\big) \\ & + \int_Z [(X_k + S_k\gamma_1(u) + I_k\gamma_2(u) \\ & + R_k\gamma_3(u))^p - X_k^p]\tilde{N}(\mathrm{d}t,\mathrm{d}u). \end{aligned}$$

Let

$$b = \eta - \frac{p-1}{2}\sigma_{\max}^2 - \frac{1}{p}\int_Z [(1+\gamma_{\max}(u))^p - 1]\nu(\mathrm{d}u) > 0,$$

where $\sigma_{\max} = \sigma_1 \vee \sigma_2 \vee \sigma_3$ and $\gamma_{\max} = \gamma_1 \vee \gamma_2 \vee \gamma_3$, then

$$\begin{aligned} LV \;\le\; & pX_k^{p-1}(t)(A - \eta X_k) + \frac{p(p-1)X_k^{p-2}(t)}{2}\left(\sigma_1^2 S_k^2(t) + \sigma_2^2 I_k^2(t) + \sigma_3^2 R_k^2(t)\right) \\ & + \int_Z X_k^p(t)[(1+\gamma_{\max}(u))^p - 1 - p(\gamma_1(u)\wedge\gamma_2(u)\wedge\gamma_3(u))]\nu(\mathrm{d}u) \\ \le\; & pX_k^{p-2}(t)\left\{AX_k - \eta X_k^2 + \frac{p-1}{2}\sigma_{\max}^2 X_k^2(t) + \frac{1}{p}\int_Z X_k^2(t)[(1+\gamma_{\max}(u))^p - 1]\nu(\mathrm{d}u)\right\} \\ =\; & pX_k^{p-2}(t)\left\{AX_k - X_k^2(t)\left[\eta - \frac{p-1}{2}\sigma_{\max}^2 - \frac{1}{p}\int_Z [(1+\gamma_{\max}(u))^p - 1]\nu(\mathrm{d}u)\right]\right\} \\ =\; & pX_k^{p-2}(t)\left(AX_k - bX_k^2(t)\right). \end{aligned} \tag{6}$$

It implies that

$$\begin{aligned} & \mathrm{d}V(X_k(t)) \\ \le\; & pX_k^{p-2}(t)\left(AX_k - bX_k^2(t)\right)\mathrm{d}t \\ & + pX_k^{p-1}(t)(\sigma_1 S_k\,\mathrm{d}B_1(t) \\ & + \sigma_2 I_k\,\mathrm{d}B_2(t) + \sigma_3 R_k\,\mathrm{d}B_3(t)) \\ & + \int_Z X_k^p(t)[(1+\gamma_{\max}(u))^p - 1]\tilde{N}(\mathrm{d}t,\mathrm{d}u). \end{aligned} \tag{7}$$

For any $i \in \mathbb{R}_+$,

$$\begin{aligned} & d\,\mathrm{e}^{it}V(X_k(t)) \\ \le\; & L[\mathrm{e}^{it}V(X_k)]\mathrm{d}t + \mathrm{e}^{it}pX_k^{p-1}(t)(\sigma_1 S_k\,\mathrm{d}B_1(t) \\ & + \sigma_2 I_k\,\mathrm{d}B_2(t) + \sigma_3 R_k\,\mathrm{d}B_3(t)) \\ & + \mathrm{e}^{it}X_k^p(t)\int_Z [(1+\gamma_{\max}(u))^p - 1]\tilde{N}(\mathrm{d}t,\mathrm{d}u). \end{aligned}$$

Integrating the inequality above from 0 to t results in

$$\begin{aligned} & \int_0^t \mathrm{d}\,\mathrm{e}^{it}V(X_k(t)) \\ \le\; & \int_0^t \left[i\mathrm{e}^{is}V(X_k(s)) + \mathrm{e}^{is}LV(X_k(s))\right]\mathrm{d}s \\ & + \int_0^t \mathrm{e}^{it}pX_k^{p-1}(t)(\sigma_1 S_k\,\mathrm{d}B_1(t) \\ & + \sigma_2 I_k\,\mathrm{d}B_2(t) + \sigma_3 R_k\,\mathrm{d}B_3(t)) \\ & + \int_0^t \mathrm{e}^{is}X_k^p(s)\int_Z [(1+\gamma_{\max}(u))^p - 1]\tilde{N}(\mathrm{d}t,\mathrm{d}u). \end{aligned}$$

Taking the expectation on both sides and applying Lemma 2, there is

$$\begin{aligned} & E\left[\mathrm{e}^{it}V(X_k(t))\right] \\ \le\; & V(X_k(0)) + E\left[\int_0^t \left[i\mathrm{e}^{is}X_k^p(s) + \mathrm{e}^{is}LV(X_k(s))\right]\mathrm{d}s\right]. \end{aligned}$$

When $0 < i < bp$, let

$$\begin{aligned} 0 \;<\; H =\; & \sup_{X_k\in\mathbb{R}_+}\left\{X_k^{p-2}(t)\left[AX_k(t) - (b - i/p)X_k^2(t)\right] + 1\right\} \\ <\; & \infty, \end{aligned}$$

we obtain

$$\begin{aligned} & i\mathrm{e}^{it}X_k^p(t) + \mathrm{e}^{it}LV(X_k(t)) \\ \le\; & i\mathrm{e}^{it}X_k^p(t) + \mathrm{e}^{it}pX_k^{p-2}(t)\left(AX_k - bX_k^2(t)\right) \\ =\; & p\mathrm{e}^{it}X_k^{p-2}(t)\left[AX_k(t) - (b - i/p)X_k^2(t)\right] \\ \le\; & p\mathrm{e}^{it}H. \end{aligned}$$

Therefore,

$$\begin{aligned} E\left[\mathrm{e}^{it}V(X_k(t))\right] \;\le\; & X_k^p(0) + E\left[pH\int_0^t \mathrm{e}^{is}\mathrm{d}s\right] \\ =\; & X_k^p(0) + \frac{pH}{i}(\mathrm{e}^{it} - 1) \\ \le\; & X_k^p(0) + \frac{pH}{i}\mathrm{e}^{it}. \end{aligned}$$

Then, for $\forall t \ge 0$,

$$E[V(X_k(t))] \le X_k^p(0) + pH := M_2. \tag{8}$$

Taking the expectation after integrating the inequality (8) from 0 to t, for any $i = 1,2,\ldots$ and sufficiently small $\delta > 0$, results in

$$\begin{aligned} & E\left[\sup_{i\delta\le t\le(i+1)\delta} X_k^p(t)\right] \\ \le\; & E\left[X_k^p(i\delta)\right] + F_1 + F_2 \le M_2 + F_1 + F_2. \end{aligned}$$

Here,

$$F_1 \;=\; E\left[\sup_{i\delta\le t\le(i+1)\delta}\left|\int_{i\delta}^t pX_k^{p-2}(s)\left(AX_k(s) - bX_k^2(s)\right)\mathrm{d}s\right|\right]$$

$$\leq E\left[\sup_{i\delta\leq t\leq(i+1)\delta}\left|\int_{i\delta}^{t} pX_k^p(s)\,(A-b)\,\mathrm{d}s\right|\right]$$
$$\leq p\,|A-b|\,E\left[\left|\int_{i\delta}^{i+1)\delta} X_k^p(s)\,\mathrm{d}s\right|\right]$$
$$\leq pA\delta E\left[\sup_{i\delta\leq t\leq(i+1)\delta} X_k^p(t)\right],$$

and

$$\begin{aligned}
F_2 &= E\left[\sup_{i\delta\leq t\leq(i+1)\delta}\left|\int_{i\delta}^{t} pX_k^{p-1}(t)\,(\sigma_1 S_k\,\mathrm{d}B_1(t)+\sigma_2 I_k\,\mathrm{d}B_2(t)+\sigma_3 R_k\,\mathrm{d}B_3(t))\right.\right.\\
&\quad\left.\left.+\int_{i\delta}^{t} X_k^p(s)\int_Z[(1+\gamma_{\max}(u))^p-1]\tilde{N}(\mathrm{d}s,\mathrm{d}u)\right|\right]\\
&\overset{(i)}{\leq} 3\sqrt{32}p\sigma_{\max}E\left[\int_{i\delta}^{(i+1)\delta}\left|X_k^p(s)\right|^2\mathrm{d}s\right]^{\frac{1}{2}}+E\left[\left|\int_{i\delta}^{t} X_k^p(s)\int_Z[(1+\gamma_{\max}(u))^p-1]N(\mathrm{d}s,\mathrm{d}u)\right|\right]\\
&\quad+E\left[\left|\int_{i\delta}^{t} X_k^p(s)\int_Z[(1+\gamma_{\max}(u))^p-1]\nu(\mathrm{d}u)\right|\right]\\
&\leq 3\sqrt{32}p\sigma\delta E\left[\sup_{i\delta\leq t\leq(i+1)\delta} X_k^p(t)\right]+2\delta E\left[\sup_{i\delta\leq t\leq(i+1)\delta} X_k^p(t)\right]\int_Z|(1+\gamma_{\max}(u))^p-1|\nu(\mathrm{d}u).
\end{aligned}$$

Thus,

$$E\left[\sup_{i\delta\leq t\leq(i+1)\delta} X_k^p(t)\right]\leq M_2+E\left[\sup_{i\delta\leq t\leq(i+1)\delta} X_k^p(t)\right]\left[pA\delta+3\sqrt{32}p\sigma\delta+2\delta\int_Z|(1+\gamma_{\max}(u))^p-1|\nu(\mathrm{d}u)\right].$$

Specifically, choose a sufficiently small $\delta>0$ such that

$$pA\delta+3\sqrt{32}p\sigma\delta+2\delta\int_Z|(1+\gamma_{\max}(u))^p-1|\nu(\mathrm{d}u)<\frac{1}{2}.$$

Hence, $E\left[\sup_{i\delta\leq t\leq(i+1)\delta} X_k^p(t)\right]\leq 2M_2$. For $\forall\varepsilon>0$, using Chebyshev's inequality[26] there is

$$\mathbb{P}\left(\sup_{i\delta\leq t\leq(i+1)\delta} X_k^p(t)>(i\delta)^{1+\varepsilon}\right)\leq\frac{2M_2}{(i\delta)^{1+\varepsilon}},$$

then applying Borel–Cantelli lemma[26] for almost all $\omega\in\Omega$, $\sup_{i\delta\leq t\leq(i+1)\delta} X_k^p(t)\leq(i\delta)^{1+\varepsilon}$.

Thereby, the existence of $i_0(\omega)$ under $i\delta\leq t\leq(i+1)\delta$ leads to $i>i_0$,

$$\frac{\ln X_k^p(t)}{\ln t}\leq 1+\varepsilon\mathbb{P}-a.e.$$

When $\varepsilon\to\infty$ and $p>1$,

$$\limsup_{t\to\infty}\frac{\ln X_k(t)}{\ln t}\leq\frac{1}{p}\mathbb{P}-a.e.$$

Namely, for sufficiently small $0<\xi<1-\frac{1}{p}$, the appearance of $T=T(\omega)$ such that for $\forall t\geq T$,

$$\ln X_k(t)\leq\left(\frac{1}{p}+\xi\right)\ln t.$$

Consequently,

$$\limsup_{t\to\infty}\frac{X_k(t)}{t}\leq\limsup_{t\to\infty}\frac{t^{\frac{1}{p}+\xi}}{t}=0\ \ \mathbb{P}-a.e.$$

Corollary 1 For any $k=1,2,\ldots n$, if $(S_k(t),I_k(t),R_k(t))\in\mathrm{R}_+^{3n}$ is the solution of model (4) with initial value $(S_k(0),I_k(0),R_k(0))\in\mathrm{R}_+^{3n}$, then

$$\lim_{t\to\infty}\frac{S_k(t)}{t}=\lim_{t\to\infty}\frac{I_k(t)}{t}=\lim_{t\to\infty}\frac{R_k(t)}{t}=0\ \ \mathbb{P}-a.e.$$

Lemma 3 For $\forall k=1,2,\ldots n$ and $p>2$, if $(S_k(t),I_k(t),R_k(t))\in\mathrm{R}_+^{3n}$ is the solution of model (4) with initial value $(S(0),I(0),R(0))\in\mathrm{R}_+^{3}$, then

$$\begin{aligned}
&\lim_{t\to\infty}\frac{\int_0^t S_k(s)\,\mathrm{d}B_1(s)}{t}=0,\\
&\lim_{t\to\infty}\frac{\int_0^t\int_Z\gamma_1(u)S_k(s)\tilde{N}(\mathrm{d}s,\mathrm{d}u)}{t}=0\ \ \mathbb{P}-a.e.,\\
&\lim_{t\to\infty}\frac{\int_0^t I_k(s)\,\mathrm{d}B_2(s)}{t}=0,\\
&\lim_{t\to\infty}\frac{\int_0^t\int_Z\gamma_2(u)I_k(s)\tilde{N}(\mathrm{d}s,\mathrm{d}u)}{t}=0\ \ \mathbb{P}-a.e.,\\
&\lim_{t\to\infty}\frac{\int_0^t R_k(s)\,\mathrm{d}B_3(s)}{t}=0,\\
&\lim_{t\to\infty}\frac{\int_0^t\int_Z\gamma_3(u)R_k(s)\tilde{N}(\mathrm{d}s,\mathrm{d}u)}{t}=0\ \ \mathbb{P}-a.e.
\end{aligned}$$

Proof The proof is similar to Refs. [16,17], so we ignore it.

3.3. Sufficient conditions for extinction and persistence of rumor

Rumor propagation models enhance the understanding of how rumors spread within the population. In practical terms, the ability to predict the trends of rumor dissemination is critically important. For instance, in realms such as social media platforms or public safety, grasping and forecasting the spread

of rumors can enable agencies and organizations to implement timely response measures. Therefore, clarifying the conditions under which rumors either die out or continue to spread can effectively guide the design and implementation of preventive and intervention strategies.

The sufficient condition for the extinction condition of rumor will be given as follows. Denote $l = \int_Z [\ln(1+\gamma_2(u)) - \gamma_2(u)]\, v(\mathrm{d}u)$ and $\tilde{R}_0 = \frac{(\mu+\eta)R_0}{\mu+\eta+\sigma_2^2/2+l}$.

Theorem 3 The solution $(S_1(t), I_1(t), R_1(t), \ldots, S_n(t), I_n(t), R_n(t)) \in \mathrm{R}_+^{3n}$ of model (4) with initial value $(S_1(0), I_1(0), R_1(0), \ldots, S_n(0), I_n(0), R_n(0)) \in \mathbb{R}_+^{3n}$ has the following inequality:

$$\limsup_{t\to\infty} \frac{\ln\Theta(t)}{t} \le (\mu+\eta+\frac{\sigma_2^2}{2}+l)\left(\tilde{R}_0-1\right) \mathbb{P}-a.e.$$

If $\tilde{R}_0 < 1$, the rumor will extinguish.

Proof Integrating the first two differential equations of model (4) from 0 to t, then adding them, yields

$$\begin{aligned}
&\frac{S_k(t)-S_k(0)+I_k(t)-I_k(0)}{t} \\
&= A-\eta\langle S_k(t)\rangle - (\mu+\eta)\langle I_k(t)\rangle \\
&\quad +\frac{1}{t}\int_0^t\int_Z (\sigma_1 S_k(s)+\sigma_2 I_k(s))\,\mathrm{d}B(s) \\
&\quad +\frac{1}{t}\int_0^t\int_Z (\gamma_1(u)S_k(s)+\gamma_2(u)I_k(s))\tilde{N}(\mathrm{d}s,\mathrm{d}u).
\end{aligned}$$

Thus, $\langle S_k(t)\rangle = \frac{A}{\eta} - \frac{\mu+\eta}{\eta}\langle I_k(t)\rangle + \phi_k(t)$, within this

$$\begin{aligned}
\phi_k(t) \;=\; &\frac{1}{\eta}\Bigg[\frac{1}{t}\int_0^t\int_Z (\sigma_1 S_k(s)+\sigma_2 I_k(s))\,\mathrm{d}B(s) \\
&+\frac{1}{t}\int_0^t\int_Z (\gamma_1(u)S_k(s)+\gamma_2(u)I_k(s))\tilde{N}(\mathrm{d}s,\mathrm{d}u) \\
&-\frac{S_k(t)-S_k(0)+I_k(t)-I_k(0)}{t}\Bigg].
\end{aligned}$$

By Corollary 1 and Lemma 3, $\lim_{t\to\infty}\phi_k(t) = 0 \;\; \mathbb{P}-a.e.$

Next,

$$\begin{aligned}
\mathrm{d}(\ln\Theta(t)) = L(\ln\Theta(t))\mathrm{d}t + &\frac{1}{\Theta(t)\langle k\rangle}\sum_{k=1}^n kP(k)\sigma_2 I_k(t)\mathrm{d}B_2(t) \\
&+\int_Z \ln(1+\gamma_2(u))\tilde{N}(\mathrm{d}t,\mathrm{d}u)
\end{aligned}$$

and

$$\begin{aligned}
L(\ln\Theta(t)) \;=\; &\frac{1}{\langle k\rangle}\sum_{k=1}^n kP(k)\beta k S_k(t) - (\mu+\eta) \\
&-\frac{\sigma_2^2}{2\Theta^2}\sum_{k=1}^n\left(\frac{kP(k)}{\langle k\rangle}I_k(t)\right)^2 \\
&+\int_Z [\gamma_2(u)-\ln(1+\gamma_2(u))]\,v(\mathrm{d}u) \\
\le\; &\frac{1}{\langle k\rangle}\sum_{k=1}^n kP(k)\beta k S_k(t) - \left(\mu+\eta+\frac{\sigma_2^2}{2}+l\right).
\end{aligned}$$

As a result,

$$\begin{aligned}
\mathrm{d}(\ln\Theta(t)) \le &\left[\frac{1}{\langle k\rangle}\sum_{k=1}^n kP(k)\beta k S_k(t) - (\mu+\eta+\frac{\sigma_2^2}{2}+l)\right]\mathrm{d}t \\
&+\sigma_2\,\mathrm{d}B_2(t) + \int_Z \ln(1+\gamma_2(u))\tilde{N}(\mathrm{d}t,\mathrm{d}u).
\end{aligned}$$

Integrating the inequality above from 0 to t results in

$$\begin{aligned}
&\frac{\ln\Theta(t)-\ln\Theta(0)}{t} \\
&\le \frac{1}{\langle k\rangle}\sum_{k=1}^n kP(k)\beta k\langle S_k(t)\rangle - \left(\mu+\eta+\frac{\sigma_2^2}{2}+l\right) \\
&\quad +\frac{\int_0^t\sigma_2\,\mathrm{d}B_2(t)}{t} + \frac{\int_0^t\int_Z \ln(1+\gamma_2(u))\tilde{N}(\mathrm{d}s,\mathrm{d}u)}{t} \\
&= \frac{1}{\langle k\rangle}\sum_{k=1}^n kP(k)\beta k\left(\frac{A}{\eta}-\frac{\mu+\eta}{\eta}\langle I_k(t)\rangle+\phi_k(t)\right) \\
&\quad -(\mu+\eta+\frac{\sigma_2^2}{2}+l) + \frac{\int_0^t\sigma_2\,\mathrm{d}B_2(t)}{t} \\
&\quad +\frac{\int_0^t\int_Z \ln(1+\gamma_2(u))\tilde{N}(\mathrm{d}s,\mathrm{d}u)}{t} \\
&\le \frac{1}{\langle k\rangle}\sum_{k=1}^n kP(k)\beta k\left(\frac{A}{\eta}+\phi_k(t)\right) \\
&\quad -(\mu+\eta+\frac{\sigma_2^2}{2}+l) + \frac{\int_0^t\sigma_2\,\mathrm{d}B_2(t)}{t} \\
&\quad +\frac{\int_0^t\int_Z \ln(1+\gamma_2(u))\tilde{N}(\mathrm{d}s,\mathrm{d}u)}{t}.
\end{aligned}$$

Let $r = \int_0^t\int_Z \ln(1+\gamma_2(u))\tilde{N}(\mathrm{d}s,\mathrm{d}u)$, then $\langle r,r\rangle(t) = t\int_Z[\ln(1+\gamma(u))]^2\nu_2(\mathrm{d}u) < tc$. By Lemma 2, we can clearly conclude that $\lim_{t\to\infty}\frac{r(t)}{t} = 0 \;\; \mathbb{P}-a.e.$ and $\lim_{t\to\infty}\frac{B(t)}{t} = 0 \;\; \mathbb{P}-a.s.$ Thus,

$$\begin{aligned}
\limsup_{t\to\infty}\frac{\ln\Theta(t)}{t} &\le \frac{\beta A}{\eta}\sum_{k=1}^n\frac{k^2P(k)}{\langle k\rangle} - (\mu+\eta+\frac{\sigma_2^2}{2}+l) \\
&= \left(\mu+\eta+\frac{\sigma_2^2}{2}+l\right)\left(\frac{(\mu+\eta)R_0}{\mu+\eta+\frac{\sigma_2^2}{2}+l}-1\right) \\
&:= \left(\mu+\eta+\frac{\sigma_2^2}{2}+l\right)\left(\tilde{R}_0-1\right).
\end{aligned}$$

If $\tilde{R}_0 < 1$, then $\limsup_{t\to\infty}\frac{\ln\Theta(t)}{t} = 0 \;\; \mathbb{P}-a.e.$, which means the rumor disappears.

Next, the sufficient condition of rumor weakly persistent will be given.

Theorem 4 Let

$$\bar{R}_0 = \eta(\mu+\eta)R_0 \Big/ \left[(\beta k+\eta)\left(\mu+\eta+\frac{\sigma_2^2}{2}+l\right)\right].$$

The solution $(S_1(t), I_1(t), R_1(t), \ldots, S_n(t), I_n(t), R_n(t)) \in \mathrm{R}_+^{3n}$ of model (4) with initial value $(S_1(0), I_1(0), R_1(0), \ldots, S_n(0), I_n(0), R_n(0)) \in \mathbb{R}_+^{3n}$ has the following inequality:

$$\liminf_{t\to\infty}\frac{\ln\Theta(t)}{t} \ge (\mu+\eta+\frac{\sigma_2^2}{2}+l)(\bar{R}_0-1) \;\; \mathbb{P}-a.e.$$

If $\bar{R}_0 > 1$, the solution $(S_1(t),\ I_1(t),\ R_1(t), \ldots,\ S_n(t),\ I_n(t),\ R_n(t)) \in \mathrm{R}_+^{3n}$ of model (4) is weakly persistent.

Proof Suppose that $\varepsilon_1 \in (0,1)$ satisfies $P\left\{\limsup_{x\to\infty} I_k(t) < p\right\} \geq \varepsilon_1$. Integrating the first equation of model (4) from 0 to t, and by means of $\Theta(t) = \sum_{k=1}^{n} kP(k)I_k(t)/\langle k\rangle \leq 1$, we obtain

$$\begin{aligned}\frac{S_k(t)}{t} &= \frac{S_k(0)}{t} + A - \frac{\beta k}{t}\int_0^t S_k(t)\Theta(t)\,\mathrm{d}t \\ &\quad - \frac{\eta}{t}\int_0^t S_k(t)\,\mathrm{d}t + \frac{\sigma_1\int_0^t S_k(t)\,\mathrm{d}B_1(t)}{t} \\ &\quad + \frac{\int_0^t S_k(t)\int_Z \gamma_1(u)\tilde{N}(\mathrm{d}t,\mathrm{d}u)}{t} \\ &\geq \frac{S_k(0)}{t} + A - \frac{\beta k+\eta}{t}\int_0^t S_k(t)\,\mathrm{d}t \\ &\quad + \frac{\sigma_1\int_0^t S_k(t)\,\mathrm{d}B_1(t)}{t} + \frac{\int_0^t S_k(t)\int_Z \gamma_1(u)\tilde{N}(\mathrm{d}t,\mathrm{d}u)}{t}.\end{aligned}$$

Therefore,

$$\liminf_{t\to\infty}\frac{\int_0^t S_k(t)dt}{t} \geq \frac{A}{\beta k+\eta}. \tag{9}$$

Since

$$\begin{aligned}&\mathrm{d}(\ln\Theta(t)) \\ &= \left[\frac{\beta\langle k^2\rangle}{\langle k\rangle}S_k(t) - (\mu+\eta) - \frac{\sigma_2^2}{2\Theta^2}\sum_{k=1}^{n}\left(\frac{kP(k)}{\langle k\rangle}I_k(t)\right)^2\right. \\ &\quad \left. + \int_Z [\gamma_2(u) - \ln(1+\gamma_2(u))]\,\nu(\mathrm{d}u)\right]\mathrm{d}t \\ &\quad + \sigma_2\,\mathrm{d}B_2(t) + \int_Z \ln(1+\gamma_2(u))\tilde{N}(\mathrm{d}t,\mathrm{d}u).\end{aligned} \tag{10}$$

Then, dividing by t after integrating Eq. (10) from 0 to t on both sides,

$$\begin{aligned}\frac{\ln\Theta(t)}{t} &= \frac{\ln\Theta(0)}{t} + \frac{1}{t}\int_0^t\left[\frac{\beta\langle k^2\rangle}{\langle k\rangle}S_k(t) - (\mu+\eta)\right. \\ &\quad - \frac{\sigma_2^2}{2\Theta^2}\sum_{k=1}^{n}\left(\frac{kP(k)}{\langle k\rangle}I_k(t)\right)^2 \\ &\quad \left. + \int_Z [\gamma_2(u) - \ln(1+\gamma_2(u))]\,\nu(\mathrm{d}u)\right]\mathrm{d}t \\ &\quad + \frac{\int_0^t \sigma_2\,\mathrm{d}B_2(t)}{t} + \frac{\int_0^t\int_Z \ln(1+\gamma_2(u))\tilde{N}(\mathrm{d}t,\mathrm{d}u)}{t} \\ &\geq \frac{\ln\Theta(0)}{t} + \frac{\beta\langle k^2\rangle}{\langle k\rangle}\frac{A}{\beta k+\eta} - \left(\mu+\eta+\frac{\sigma_2^2}{2}+l\right) \\ &\quad + \frac{\int_0^t \sigma_2\,\mathrm{d}B_2(t)}{t} + \frac{\int_0^t\int_Z \ln(1+\gamma_2(u))\tilde{N}(\mathrm{d}t,\mathrm{d}u)}{t}.\end{aligned}$$

Thus, utilizing Lemma 2,

$$\begin{aligned}\liminf_{t\to\infty}\frac{\ln\Theta(t)}{t} &\geq \frac{\beta\langle k^2\rangle}{\langle k\rangle}\frac{A}{\beta k+\eta} - \left(\mu+\eta+\frac{\sigma_2^2}{2}+l\right) \\ &= \left(\mu+\eta+\frac{\sigma_2^2}{2}+l\right)(\bar{R_0}-1).\end{aligned}$$

If $\bar{R}_0 > 1$, the rumor will be popular.

4. Numerical simulations

4.1. Numerical calculation

The numerical scheme of model (4) will be given by the Milstein method as follows (model (3) can be similarly derived):

$$\begin{aligned}S_k(t+1) &= S_k(t) + [A - \beta k S_k(t)\Theta(t) - \eta S_k(t)]\Delta t \\ &\quad + \sigma_1 S_k(t-)\Delta W_1(t) + 0.5\sigma_1^2 S_k(t-) \\ &\quad \times (\Delta W_1^2(t) - \Delta t) + S_k(t-)\Delta Z_1(t); \\ I_k(t+1) &= I_k(t) + [\beta k S_k(t)\Theta(t) - (\mu+\eta)I_k(t)]\Delta t \\ &\quad + \sigma_2 I_k(t-)\Delta W_2(t) + 0.5\sigma_2^2 I_k(t-) \\ &\quad \times (\Delta W_2^2(t) - \Delta t) + I_k(t-)\Delta Z_2(t); \\ R_k(t+1) &= R_k(t+1) + [\mu I_k(t) - \eta R_k(t)]\Delta t \\ &\quad + \sigma_3 R_k(t-)\Delta W_3(t) + 0.5\sigma_3^2 R_k(t-) \\ &\quad \times (\Delta W_3^2(t) - \Delta t) + R_k(t-)\Delta Z_3(t),\end{aligned}$$

where $k = 1,2,\ldots,n$ and Δt represents the scale of step within interval $[0,T]$. $\Delta W_i = \xi_i\sqrt{\Delta t}$ $(i = 1,2,3)$ represents the increment of Brownian motion, ξ_i is an independent Gaussian random variable, following a normal distribution $N(0,1)$. The discrete component of Lévy noise $Z_i(t)$, whose increments are generated by the symmetric α-stable process as follows (see Ref. [27]).

Algorithm 1: Increment of $Z_i(t)$

Generate two independent and identically distributed random variables U and V, where U is uniformly distributed over $\left[-\frac{\pi}{2},\frac{\pi}{2}\right]$, and V is uniformly distributed over $[0,\ 1]$.

Calculate $W = -\ln(V)$.

Calculate ΔZ_i $(i = 1,2,3)$, the index of stability α belongs to $(0,2)$, $\Delta Z_i(t) = \Delta t^{1/\alpha}\frac{\sin\alpha U}{(\cos U)^{1/\alpha}}\left(\frac{\cos((1-\alpha)U)}{W}\right)^{(1-\alpha)/\alpha}$.

4.1.1. Network description

The initial scale of the artificial network is $N_0 = 1000$. Suppose that the degree of nodes varies $m = 1$ to $n = 100$ on a heterogeneous network and the degree distribution obeys a power-law distribution $p(k) = \frac{(v-1)m(m+1)}{k(k+1)(k+2)} \propto (v-1)m^{(v-1)}k^{-v}$, where $v = 3$.[28] Fix the index of stability $\alpha = 1.5$. An average of 100 simulations is taken to reduce random errors and each simulation starts from randomly chosen initial infected nodes.

4.1.2. Theoretical verification

Next, three cases are given to verify the rationality of the proposed model.

Case 1 Assume that the average degree is $\langle k\rangle = 6$ on homogeneous networks. Setting the parameters as $A = 0.01$, $\beta = 0.5$, $\mu = 0.7$, $\eta = 0.08$, $\sigma_i = \gamma_i = 0.1$ for any $i = 1,2,3$, the numerical solution of model (3) is shown in Fig. 4. It is found that $I(t)$ will decrease to zero after reaching a peak as time progresses, while $S(t)$ gradually decreases to a stable level, while $R(t)$ rises to stability.

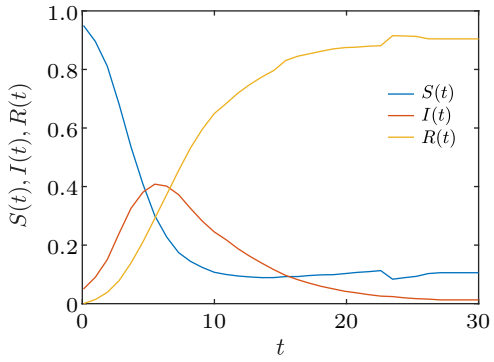


Fig. 4. Numerical scheme of model (3) under $\tilde{R}_0 < 1$.

Case 2 Setting the values of parameters as Case 1, for any $i = 1, 2, 3$, the numerical scheme of SIR propagation model in three situations, contains without noise ($\sigma_i = \gamma_i = 0$), Gaussian white noise ($\sigma_i = 0.1$, $\gamma_i = 0$) and Lévy noise ($\sigma_i = \gamma_i = 0.1$), are displayed in Fig. 5. At this time, $\tilde{R}_0 = 0.9461 < 1$. Through comparison, it can be found that Lévy noise is better at describing the suddenness present in reality.

To enhance the comparability of rumor evolution processes on homogeneous and heterogeneous networks, assume that the average degree on homogeneous networks is the same as that on heterogeneous networks. From Fig. 5, as the time of diffusion increases, the density of I nodes will quickly decrease to zero after it reaches a peak value. The density of S nodes slowly increases after rapidly decreasing due to the presence of both $I(t) = 0$ and the inflow volume A, while one of the removed nodes gradually rises to stability. Given the heterogeneity of heterogeneous networks, fluctuations caused by sudden events are more pronounced on it than on homogeneous networks.

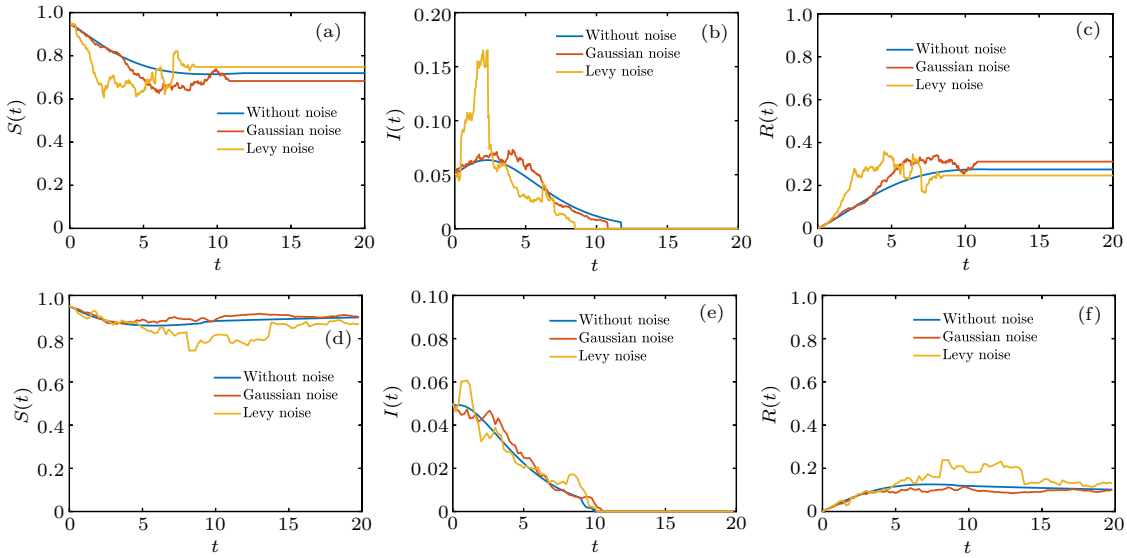


Fig. 5. Evolution of SIR propagation model with three states of noise under $\tilde{R}_0 < 1$. (a)–(c) Homogeneous networks, (d)–(f) heterogeneous networks.

Case 3 Setting parameters as $A = 0.01$, $\beta = 0.5$, $\mu = 0.01$, $\eta = 0.032$, for any $i = 1, 2, 3$, the numerical scheme of SIR propagation model in three situations, contains without noise ($\sigma_i = \gamma_i = 0$), Gaussian white noise ($\sigma_i = 0.1$, $\gamma_i = 0$) and Lévy noise ($\sigma_i = \gamma_i = 0.1$), are displayed in Fig. 6. At this time, $\bar{R}_0 = 1.4577 > 1$.

Figure 6 vividly shows that $S(t)$ rapidly decreases and gradually stabilizes. Among them, in the later stage of propagation, $S(t)$ shows an upward trend due to the increase in S-nodes is higher than the outflow. Meanwhile, $I(t)$ slowly decreases and continues to prevail after reaching its peak, while $R(t)$ shows an upward trend. The curves of the model with Gaussian white noise and Lévy noise both fluctuate up and down the deterministic model curve, and the amplitude of Lévy fluctuation is greater than Gaussian white noise, simulating the suddenness of the rumor propagation process.

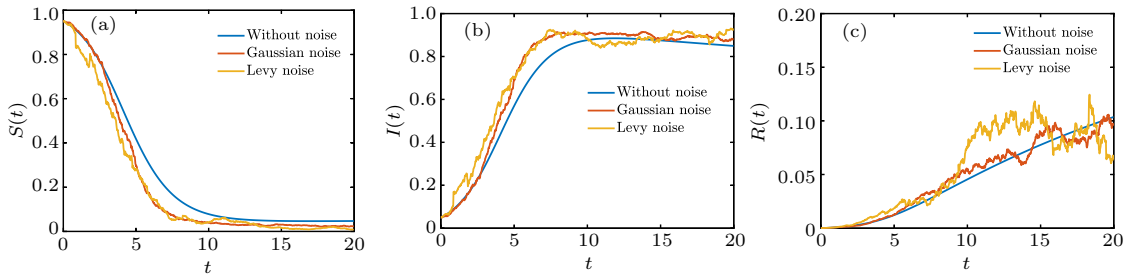


Fig. 6. Evolution of SIR propagation model with three states of noise under on heterogeneous networks.

Case 4 Here, we will discuss the special case where $\tilde{R}_0 > 1$ and $\bar{R}_0 < 1$. $A = 0.01$, $\beta = 0.5$, $\mu = 0.04$, $\eta = 0.032$, $\sigma_i = \gamma_i = 0.1$ for any $i = 1,2,3$. Here, $\tilde{R}_0 = 14.1803 > 1$ and $\overline{R_0} = \tilde{R}_0 \frac{\eta}{\beta k+\eta} \leq 0.8530 < 1$. In this scenario, as depicted in Fig. 7(a), the rumor continues to spread.

On the other hand, if we set $\mu = 0.7$ while keeping other parameters unchanged, with $\tilde{R}_0 = 1.4002 > 1$ and $\bar{R}_0 = \tilde{R}_0 \frac{\eta}{\beta k+\eta} \leq 0.0842 < 1$, the SIR evolution process, as shown in Fig. 7(b), indicates that the rumor tends to die out.

From the discussion above, it is clear that with $\tilde{R}_0 > 1$ and $\bar{R}_0 < 1$, it is not possible to definitively determine whether the rumor will die out or continue to spread. Therefore, this paper only provides sufficient conditions for the extinction and continuous spread of rumors. Specifically, the rumor will die out if $\tilde{R}_0 < 1$, while the rumor will continue to spread if $\bar{R}_0 > 1$.

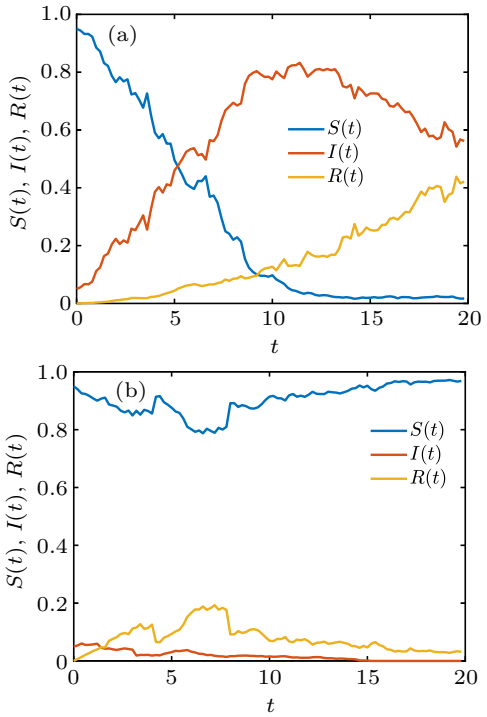


Fig. 7. Evolution of SIR propagation model with three states of noise under (a) $\tilde{R}_0 > 1$ and (b) $\tilde{R}_0 < 1$.

4.1.3. Sensitivity analysis

Sensitivity analysis is a valuable technique for determining the impact of changes in model parameters on the dynamics of propagation, particularly for estimating the expected effectiveness of rumor prevention measures. This analysis measures the impact of slight variations in the parameters of the rumor spreading model, such as the infected rate, removed rate, and outflow rate, on the numerical value of the basic reproduction number. Here, the direct differentiation method is utilized to calculate the sensitivity.

Definition 1[28] The sensitivity index H_p can be regard as the threshold parameter R_0 that depends on the parameter p as below:

$$H_p = \frac{p}{R_0} \times \frac{\partial R_0}{\partial p}. \tag{11}$$

Fixed the value of parameters as Case 2, assuming that $v(Z) = 1$, then the effects of parameters on R_0 and $\tilde{R}_0$ can be obtained as Table 2 and Fig. 8. To enhance the comprehensibility of Table 2, we provide an example of the calculation process. For instance, under the values of parameters in Case 2,

$$\begin{aligned} H_\mu &= \frac{\mu}{R_0} \times \frac{\partial R_0}{\partial \mu} = \frac{\mu}{R_0} \times \frac{-\langle k^2 \rangle \beta A}{\langle k \rangle \eta (\mu+\eta)^2} \\ &= \frac{-\mu}{\mu+\eta} = \frac{-0.7}{0.7+0.08} \approx -0.8974 \end{aligned}$$

describes the sensitivity of μ to R_0, $H_\eta = \frac{\eta}{\tilde{R}_0} \times \frac{\partial \tilde{R}_0}{\partial \eta} \approx -1.1013$ describes the sensitivity of η to $\tilde{R}_0$. Other sensitivity indices can be obtained similarly. An explanation of the values in Table 2 for R_0 and $\tilde{R}_0$ follows. It is evident to discover that the growth (or decay) of these parameters value leads to an increase (or decrease) in R_0. For instance, a 10% increase in A and β results in a corresponding 10% and 10% increase in R_0. Meanwhile, a 10% increase in μ and η results in a corresponding 8.974% and 1.026% decrease in R_0. For $\tilde{R}_0$, a 10% increase in μ, $\eta\sigma_2$ and l results in a corresponding 8.864%, 11.013%, 0.127%, and 0.059% decrease in $\tilde{R}_0$.

Table 2. Sensitivity indices of R_0 and $\tilde{R}_0$.

Parameters	S index	Value (for R_0 parameters)	Value (for $\tilde{R}_0$ parameters)
A	H_A	1.000	1.0000
β	H_β	1.000	1.0000
μ	H_μ	−0.8974	−0.8864
η	H_η	−0.1026	−1.1013
σ_2	H_{σ_2}	/	−0.0127
l	H_l	/	−0.0059

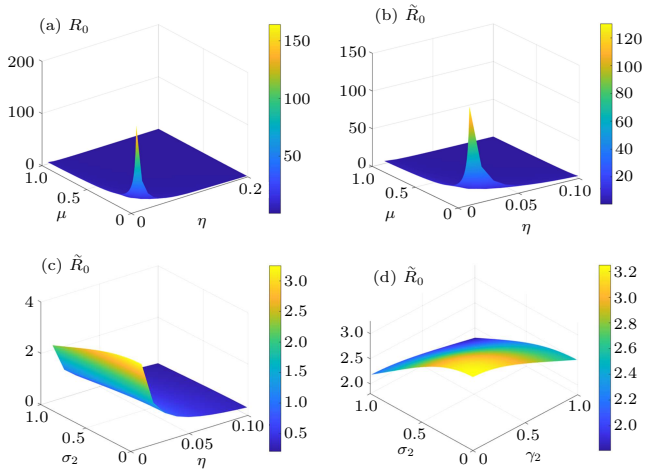


Fig. 8. Sensitivity analysis of various parameters for R_0 and $\tilde{R}_0$.

Case 5 Fixed $A = 0.01$, $\beta = 0.5$, $\eta = 0.08$, $\sigma_1 = \gamma_1 = 0.1$, $\sigma_i = \gamma_i = 0$ $(i = 2,3)$, then the diagram of model (4) with various $\mu = 0.7, 0.8, 0.9, 1$ as shown in Figs. 9(a)–9(c). In the early stages of rumor propagation, it is found that $S(t)$ decreases as

the reduction of μ, while $I(t)$ and $R(t)$ increase. In the later stage of rumor propagation, μ has little effect on $S(t)$ and $R(t)$, but $I(t)$ will decrease as μ increases.

Fixed other parameters except $\mu = 0.7$ and $\eta = 0.08$, 0.1, 0.2, 0.3, the changes diagram of SIR rumor propagation model induced by Lévy noise is illustrated in Figs. 9(d)–9(f). It is shown that as time progresses, $S(t)$ slowly decreases to a stable state, while $R(t)$ exhibits the opposite trend. $I(t)$ will rapidly rise to a peak before declining to a steady state. Moreover, a larger value of η accelerates the extinction rate of the rumors.

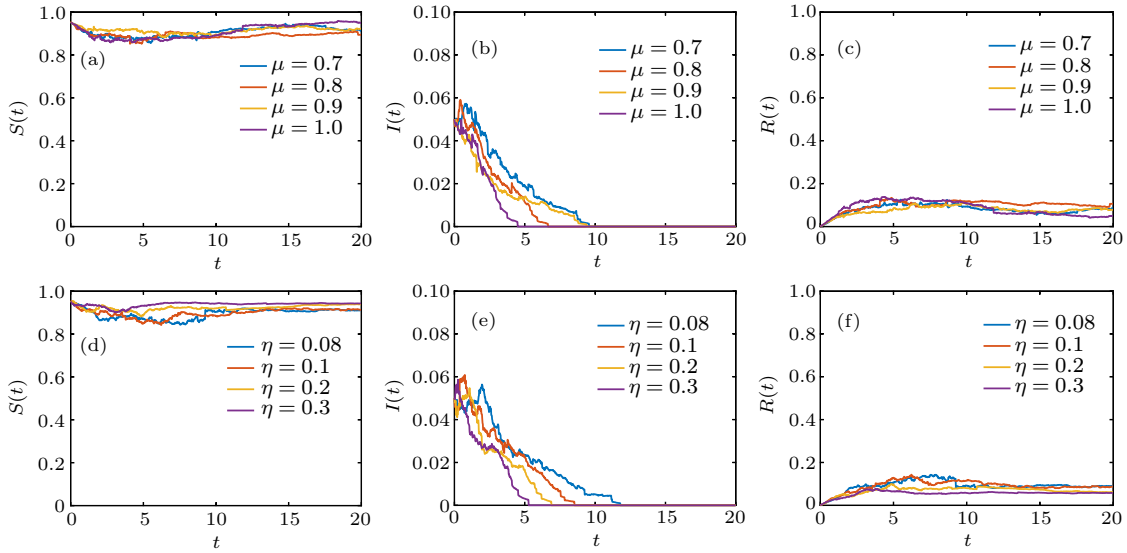


Fig. 9. Evolution of model (4) with various (a)–(c) μ and (d)–(f) η.

4.2. Simulation experiments

4.2.1. Artificial network

Assume that the average degree is $\langle k \rangle = 6$ and the rewiring probability is $p = 0.2$[11] on WS networks. On the BA network, the initial number of nodes is set as 6 with 6 growth edges, and the network average degree equals 6. All parameters are set the same as in Case 1. Figure 10 shows that the two subplots exhibit similar trends to Case 1 and Case 2. Specifically, as time progresses, $I(t)$ peaks and then gradually declines to zero, $S(t)$ slowly decreases to a stable state, and $R(t)$ simultaneously increases slowly to stability, which validates the reasonableness of the proposed model.

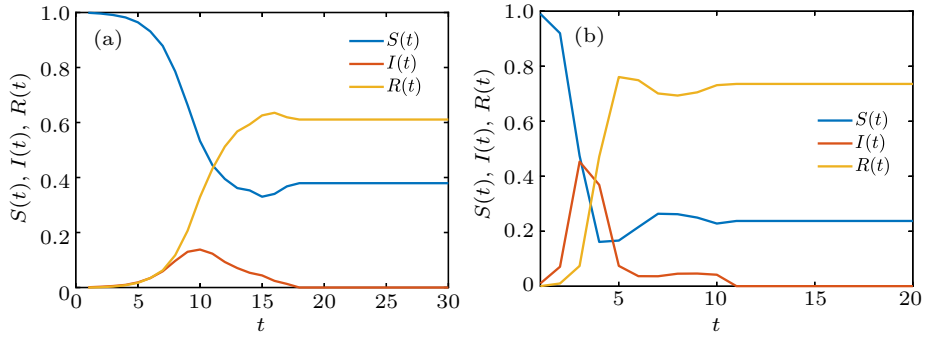


Fig. 10. Evolution of SIR model induced by Lévy noise. (a) WS networks, (b) BA networks.

4.2.2. Stochastic resonance

The threshold $\tilde{R}_0$ of model (4) is related with noise intensities σ_2 and γ_2 compared with the corresponding determination system. Two indicators, the peak density of infected nodes and the life cycle of rumor, are selected to describe the changes of system as σ_2 and γ_2 increase.

As seen in Fig. 11, increasing the noise intensities σ_2 and γ_2 suppresses the peak value and life cycle of rumor propagation. That is to say, the addition of Lévy noise can block the diffusion of rumors, which implies the occurrence of stochastic resonance on the proposed SIR rumor propagation model with Lévy noise. Consequently, we can apply appropriate levels of noise intensity to control the spread of rumors. This requires finding the optimal noise intensity to minimize the scale of rumor dissemination. Next, we will explore the effects of different noise intensities on the peak and life cycle of rumors on WS and Barabási–Albert (BA) networks.

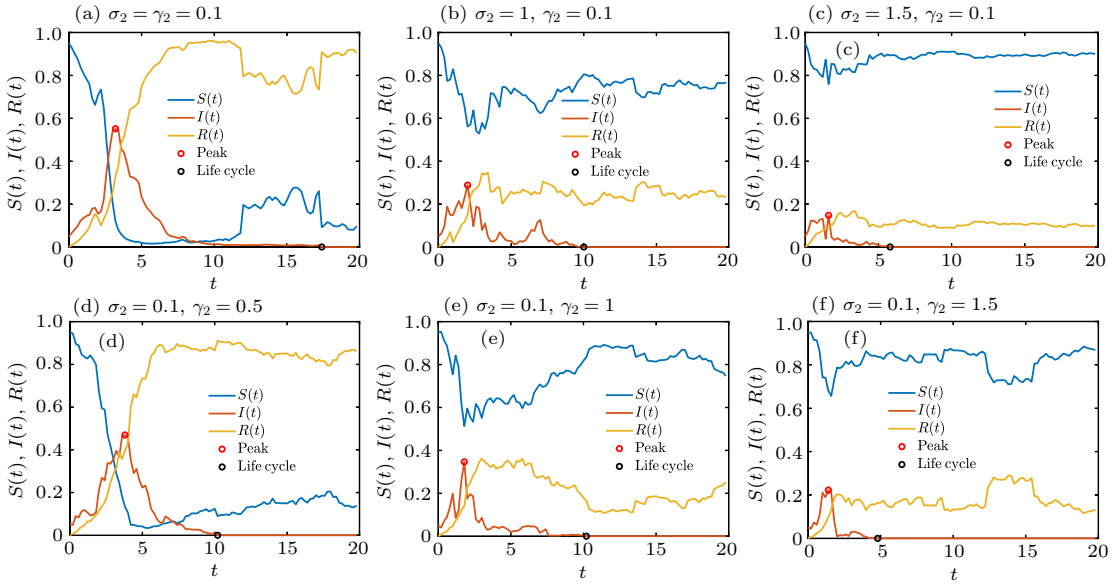


Fig. 11. Evolution of SIR model induced by Lévy noise with various σ_2 and γ_2 on heterogeneous networks.

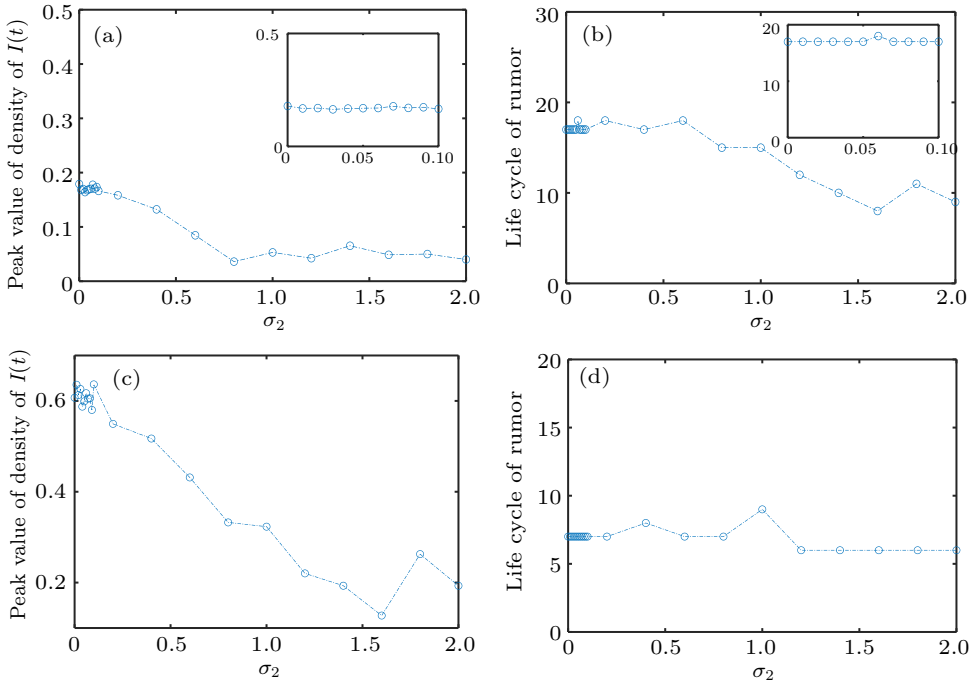


Fig. 12. The peak density of $I(t)$ and life cycle of rumor under different σ_2. (a), (b) WS networks; (c), (d) BA networks.

Figure 12 vividly illustrates the changes in the peak and life cycle of rumor spread on WS and BA networks, driven by varying noise intensities σ_2. It is observed that an increase in noise intensity σ_2 leads to a reduction in both the peak and life cycle of rumors, thereby suppressing the spread of rumors. Figure 13 further explores the effects of simultaneous changes in noise intensities σ_2 and γ_2 on the peak and life cycle of rumors, revealing that σ_2 plays a dominant role in curbing the spread of rumors.

To better harness the phenomenon of stochastic resonance for suppressing rumor propagation, we need to identify the optimal noise intensity that minimizes the scale of rumor spread. Taking the WS network as an example, the objective function is defined as the sum of the peak and lifespan of the rumors, which we aim to minimize,

$$\min J = \max(I(t)) + t_{I(t)=0}.$$

Here, $\max(I(t))$ represents the peak value of rumor spread, $t_{I(t)=0}$ represents the moment when the rumor first reaches zero, signifying the extinction time, which is used to denote the life cycle of the rumor. Based on the data obtained from the simulation experiments in Fig. 13(b), we find that $\min J = 3.2648$ when the noise intensities $\sigma_2 = 1.7$ and $\gamma_2 = 2.4$, at which point the peak density of $I(t)$ is 0.0348 and the life cycle of rumor is 3.23.

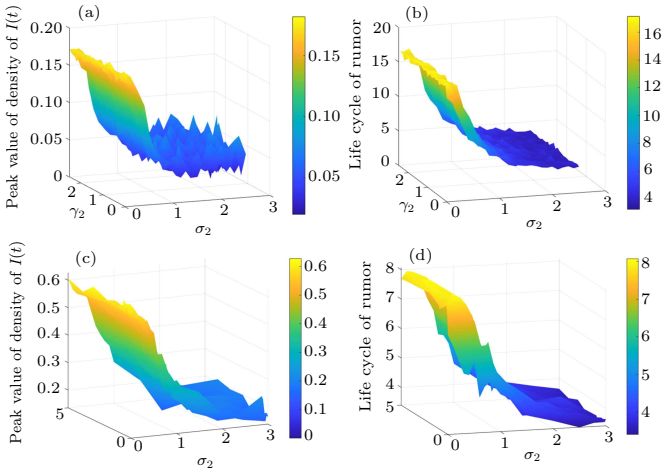


Fig. 13. The peak density of $I(t)$ and life cycle of rumor under different σ_2 and γ_2. (a), (b) WS networks; (c), (d) BA networks.

4.3. Real dataset verification

To verify the effectiveness of the proposed model, we randomly selected Dataset_R2, Dataset_R5, and Dateset_R7 from the 12 datasets of newly emerged rumors in Twitter collected by Amirhosein (https://zenodo.org/records/2563864). In Dataset_R2, Dataset_R5, and Dataset_R7, 497 users, 181 users and 690 users posted tweets related to the rumor, respectively, during the spread of the rumor. We only record users who retweeted rumor-related posts as infected state. Users who viewed and believed the rumor but did not tweet about it are not recorded. Then, set the unit time to one hour for processing the real dataset.

The sum of squares error (SSE) is used to judge the fitting effect of the proposed stochastic SIR model with real data. That is,

$$\mathrm{SSE} = \sum_{t=1}^{\infty} (y_t - I(t))^2,$$

where y_t implies the real value at moment t and $I(t)$ represents the estimated value according to the proposed model. It should be emphasized that a lower value of SSE indicates a more effective fit. Thus, the particle swarm optimization (PSO) algorithm is utilized to obtain a better fitted value. Set the inertia factor $w = 0.9$ and the acceleration constants $c_1 = c_2 = 2$ of the PSO algorithm. Meanwhile, let the number of particle swarm be 1000 and the maximum number of iterations be 100.

When the system receives noise interference, it is assumed that $A = 0.01$ and each individual in the system is affected by the same intensity of the noise. Thus, the values of the optimal parameters can be found by PSO algorithm under the minimum SSE, as displayed in Table 3 and the fitting effect is vividly displayed in Fig. 14. It is evident that in the early stages of rumor propagation, the proposed model effectively fits the real dataset. However, in the later stages of rumor spread, the density of infected individuals fluctuates near zero, likely due to internal system dynamics or other uncertainties.

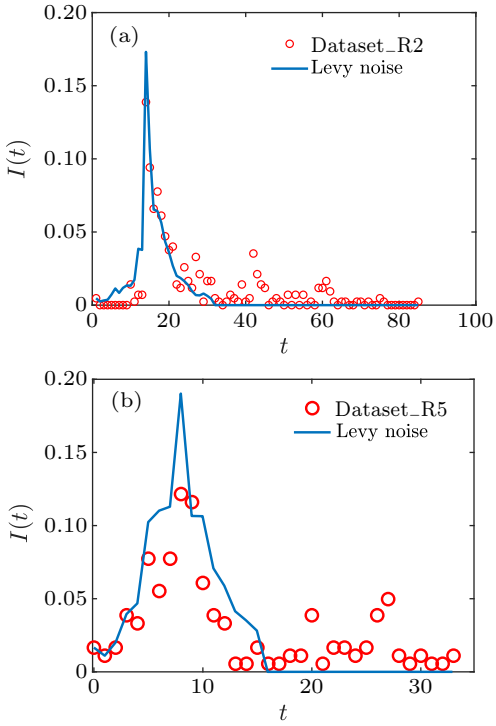


Fig. 14. Fitting diagram of real dataset and the proposed model.

Table 3. Values of optimal parameters by PSO algorithm.

Real dataset	β	μ	η	σ_i	γ_i	Fitness value
Dateset_R2	0.941	0.005	0.345	0.086	0.03	0.0557
Dateset_R5	0.861	0.083	0.063	0.021	0.098	0.0232

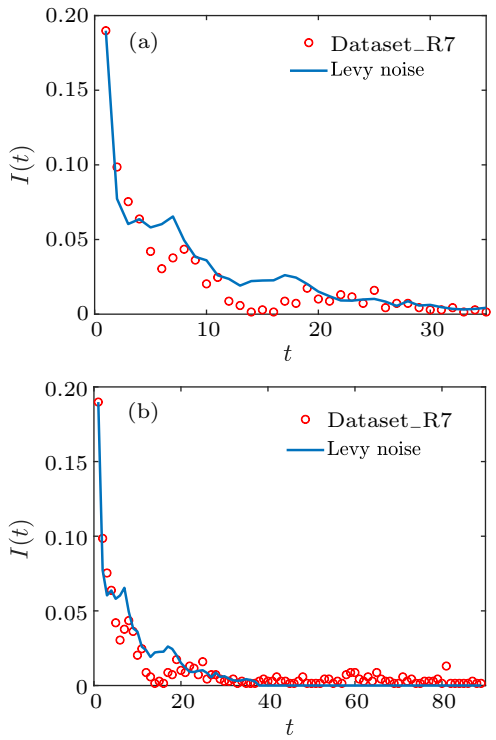


Fig. 15. Fitting diagram of Dataset_R7 and the proposed model.

After processing, Dataset_R7 comprises 89 data points. Using the proposed model, we fit the first 40% of the data and obtain the parameter values as shown in Table 4. From the

trend of changes in the real dataset, it can be seen that the infected individuals in the population are saturated, so the infection rate and immunity rate are taken as 0. Then, we make the prediction and compare the trend of proposed model with the latter 60% of the data. As illustrated in Fig. 15, the proposed model can accurately predict the trend of the real data.

Table 4. Values of optimal parameters by PSO algorithm.

Real dataset	β	μ	η	σ_i	γ_i	Fitness value
Dateset_R7	0	0	0.069	0.078	0.1	0.0053

5. Conclusion

In this paper, we consider the disturbance of inflow rate, represented by Lévy noise, which better captures the variability and suddenness in the real world. Based on this, we propose a more comprehensive rumor propagation model. With the intent to demonstrate the stability of this model, a unique positive global solution is derived by the Lyapunov method on heterogeneous networks. Then, the asymptotic path-wise estimation of this solution and the sufficient conditions for rumor extinction and persistence are obtained on heterogeneous networks. Subsequently, simulation experiments are conducted in both artificial and real-world networks, which have validated the accuracy of the theory. Then, sensitivity analysis on the parameters of the threshold value is conducted. In addition, we discover that the Lévy noise can suppress the spread of negative rumors. On this basis, the local optimal noise intensities are obtained by the minimum of both the peak densities of infected nodes and life cycle of rumor on WS networks. Finally, the effectiveness of the proposed model is verified on three real datasets by PSO algorithm.

As a future research direction, we are inclined to consider other dynamic property of stochastic SIR model and explore the stochastic resonance in nonlinear systems.

Acknowledgements

This work is supported in part by the National Natural Science Foundation of China (Grant Nos. 62071248 and 62201284) and in part by the Graduate Scientific Research and Innovation Program of Jiangsu Province (Grant No. KYCX24_1119).

References

[1] Arnold L, Horsthemke W and Stucki J 1979 *Biomedical Journal* **21** 451
[2] Ludwig D 1975 *SIAM Review* **17** 605
[3] Beddington J R and May R M 1977 *Science* **197** 463
[4] Truscott J E and Gilligan C A 2003 *Proc. Natl. Acad. Sci. USA* **100** 9067
[5] Bobryk R V 2021 *Chaos Solitons & Fractals* **143** 110552
[6] Liu M and Wang K 2013 *Discrete and Continuous Dynamical Systems* **33** 2495
[7] Zhang Y H and Zhu J J 2022 *Chin. Phys. B* **31** 060202
[8] Mao X R, Marion G and Renshaw E 2002 *Stochastic Processes and their Applications* **97** 95
[9] Jiang D Q, Yu J J, Ji C Y and Shi N Z 2011 *Mathematical and Computer Modelling* **54** 221
[10] Zhu L and Wang Y G 2017 *Physica A* **469** 750
[11] Chai Y, Wang Y G and Zhu L 2019 *IEEE Access* **7** 175897
[12] Tong X R, Jiang H J, Qiu J L, Luo X P and Chen S S 2023 *Chaos, Solitons & Fractals* **173** 113637
[13] Zhang X and Wang K 2013 *Applied Mathematics Letters* **26** 867
[14] Applebaum D 2009 *Lévy Processes and Stochastic Calculus* (2st edition) (New York: Cambridge University Press) pp. 355–394
[15] Bao J H and Yuan C G 2012 *Journal of Mathematical Analysis and applications* **391** 363
[16] Zhou Y L and Zhang W G 2016 *Physica A* **446** 204
[17] Privault N and Wang L 2021 *Journal of Nonlinear Science* **31** 1
[18] Huo L A, Dong and Lin T T 2021 *Chin. Phys. B* **30** 080201
[19] Huo L A and Dong Y F 2022 *Chin. Phys. B* **31** 030202
[20] Mcnamara B and Wiesenfeld K 1989 *Phys. Rev. A* **39** 4854
[21] Liu J, Wang Y G and Zhai Q Q 2016 *IEICE Transactions on Fundamentals of Electronics Communications and Computer Sciences* **E99** 323
[22] Guo Y, Wan L, Wei F and Tan J 2020 *Indian Journal of Physics* **94** 1625
[23] Barbay S, Giacomelli G and Marin F 2000 *Phys. Rev. E* **61** 157
[24] Dunkel J, Hilbert S, Schimansky-Geier L and Hanggi P 2004 *Phys. Rev. E* **69** 056118
[25] Sun X L, Wang Y G and Cang L Q 2022 *Chin. Phys. B* **31** 050202
[26] Mao X R 2007 *Stochastic differential equations and applications*, 2nd Edn. (United Kingdom: Woodhead Publishing Limited) pp. 9–48
[27] Jum E 2015 *Numerical approximation of stochastic differential equations driven by Lévy motion with infinitely many jumps* (PhD dissertation) (Knoxville: University of Tennessee)
[28] Zafar Z U A, DarAssi M H, Ahmad I, Assiri T A, Meetei M Z, Khan M A and Hassan A M 2023 *Results in Physics* **53** 106995